

A central pattern generator approach to footstep transition for biped navigation

Zeyang Xia^{1,2}, Hao Deng^{1,2}, Xue Zhang^{1,2}, Shaokui Weng^{1,2},
Yangzhou Gan^{1,2}, and Jing Xiong¹

Abstract

Existing sampling-based footstep planning method for biped navigation used an intermediate static posture for footstep transition. However, when adopting this approach, the robot is sensitive to modeling error and external environments, and also the transition between different gait patterns is unnatural. This article presents a central pattern generator approach to footstep transition for biped navigation. First, this approach decomposes the biped walking motion into five motion types and designs central pattern generator network for all joints of legs accordingly. Then, the central pattern generator parameters are simplified and the relationship between these parameters and footstep transition is formulated. By modifying the central pattern generator parameters, different walking gaits can be obtained. With sensing feedbacks, self-adaption walking on irregular terrains, such as walking on unknown sloped terrains and flat floor with tiny obstacles, is realized. Experiments were conducted both in simulator and on a physical biped robot. Results have shown that the proposed approach is able to generate gesture transition trajectory for biped robot navigation and realize a self-adaption walking for irregular terrains.

Keywords

Biped walking, footstep planning, central pattern generator, environment learning, self-adaption

Date received: 9 August 2016; accepted: 27 October 2016

Topic: Special Issue - Robotic Applications Based on Deep Learning

Topic Editor: Hesheng Wang

Introduction

With better mobility and an anthropoid shape, biped robots are expected to assist human activities in daily environment, such as offices, hospitals, or at homes. To execute senior tasks in human-living environments, an effective footstep planning method for biped navigation is increasingly demanded.

Previous navigation methods for biped robots can be roughly classified into two aspects. The first method is a deterministic sampling-based footstep planning, which is effective in open environments.^{1–3} The second method is a random sampling-based method to goal-bias the footstep planning, which can accomplish navigation in some special environments, such as fields with local minimal or narrow

passages.^{4–6} Since human-living environment is complex and varied, in many research, the second method has been used for humanoid robot global navigation.

The framework for biped robot navigation is normally composed of three parts, as shown in Figure 1. The first

¹ Shenzhen Institutes of Advanced Technology, Chinese Academy of Sciences, Shenzhen, China

² Laboratory of Human-Machine Intelligence-Synergy Systems, Chinese Academy of Sciences, Shenzhen, China

Corresponding author:

Zeyang Xia and Jing Xiong, 1068 Xueyuan Avenue, Shenzhen University Town, Shenzhen, China.

Emails: zy.xia@siat.ac.cn, jing.xiong@siat.ac.cn



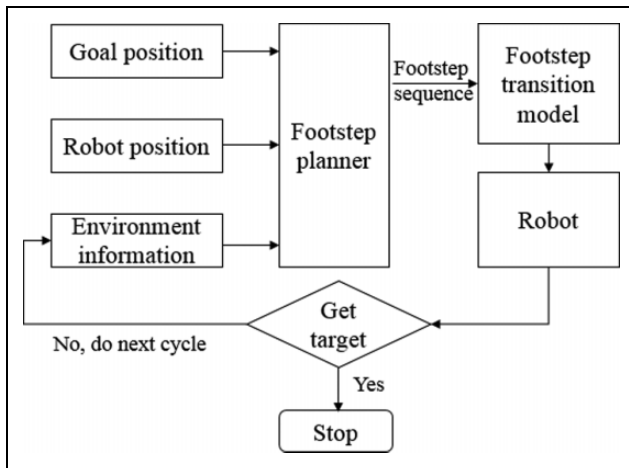


Figure 1. Sampling-based footstep planner for biped robots.⁴

section is the environment sensing (Kinect used), which is used to get the surrounding environment. The second section is a randomized search tree, which can generate footstep sequences. And the last section is a footstep transition model, which supplies an element footstep library as the searching manifold. Intermediate static posture (ISP) is a traditional footstep transition model that is planned offline and used online.⁶ Although ISP could decrease the computation complexity, the step is processed in advance and sometimes the transition between different gaits seemed to be unnatural.

Biological studies of animals suggest that the central pattern generator (CPG) existing at the spinal cord combined with reflexes receiving adjusting signals from the cerebrum and the brain controls the animals motion (such as walking, heartbeat, and breathing).⁷ CPG control methodology was built to accomplish the similar function of CPG in animals, and this methodology has become a powerful tool for generating a locomotion pattern for biped robot in recent years.^{8–11} CPG control methodology usually does not need precise robot model and makes walking motion be more natural. Since the CPG can combine with feedback signals easily, many adaptive locomotion has been obtained based on the CPG method. In order to address those issues of current methods using ISP, CPG was used in our work to provide an effective and adaptive gesture transition trajectory for biped robot navigation.

However, tuning parameters of the CPG method is a difficult task for biped robot navigation because of a large number of parameters and the lack of relationship mapping between parameters and dynamic behaviors. So, our subjects in this research are (1) providing an effective gesture transition trajectory for robot footstep planning. Different walking gaits were obtained, which contain walking forward, backward, lateral, and rotation; (2) simplifying the parameters of CPG and building a certain relationship between the parameters of CPG and the position of swing foot; (3) changing parameters of CPG by values of sensors to adapt the irregular terrains.

The rest of this article is organized as follows. The section “Gesture transition trajectory based on CPG”

describes the role of CPG in the footstep planning and the process of generation CPG. The results of experiments conducted both in simulator and physical robot are given in section “Experiments.” At last, the conclusion of this article along with a discussion on our future work is given in section “Conclusion and future work.”

Gesture transition trajectory based on CPG

In order to adopt the CPG method to generate gesture transition trajectory for the biped robot navigation, the corresponding relationship between CPG parameters and the locomotion should be constructed. After getting the footstep sequences, relationship would be required to directly guide the position of the landing foot. There are two kinds of CPG control approaches: to allocate CPG units at each joints of the legs to demonstrate desired locomotion or to allocate CPG units to partial variables to simulate periodic characteristics of walking gait.¹² No matter what kind of CPG control approach we take, the relationship between the parameters of CPG and the locomotion is not clear, and it is hard to obtain a sequence footstep.

In this study, we aimed to build a CPG control method for biped robot and obtain corresponding relationship between the parameters of CPG and the locomotion. So, first, we will analyze the attribute of walking motion, and on this basis, the CPG oscillators will be built. After that, adaptive walking with feedback will be obtained.

Although many kinds of biped robots have been developed nowadays, such as ASIMO, ATLAS, QRIO, and NAO, they still share some common features. Taking NAO as the example, physically this biped robot has two arms and two legs. Each leg has six actuated degrees of freedoms (DOFs), and functionally all DOFs can be classified into three kinds, the first kind is responsible for leg abduction/adduction (lateral hip and ankle joints), the second kind for leg extension/flexion (sagittal hip, knee, and ankle joint), and the third kind for leg intorsion/extorsion (frontal hip joint). As arms have a little assistant for walking, typically in the research of biped working, the arms would not be considered. So in our current study, when robot walks, upper body of the biped robot is expected to keep in an upright position. Thus, in Figure 2(a), the joint diagram of a simplified biped robot with $N=12$ actuated DOFs is shown. Figure 2(b) gives the notations for the joint angles, which will be named for joint navigation in the rest of this article.

In our research, we modeled the basic walking locomotion of biped robot into five types of motion in the three planes according to the motion attribute, as shown in Figure 3.

Trajectory regulator

To generate any footsteps for biped robot walking, we need to construct a trajectory regulator for each motion types.

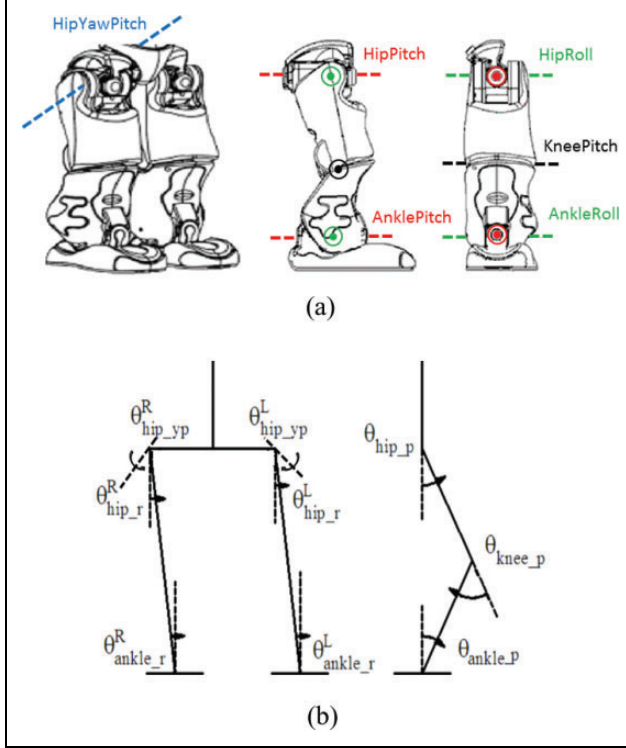


Figure 2. Biped robot model. (a) The lower limb joints of a biped robot.¹³ (b) Notations for joint angles.

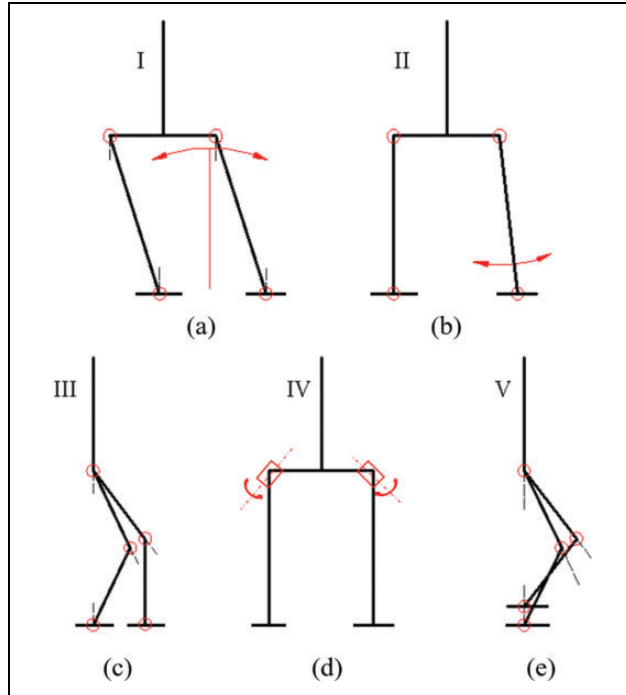


Figure 3. Five motion types of basic walking locomotion. (a). Side-to-side motion (I), (b) stepping side motion (II), (c) forward motion (III), (d) rotating motion (IV), and (e) lifting motion (V).

Motion types in lateral plane. There are two types of motion in lateral plane, the side-to-side motion-I (Figure 3(a)) and stepping side motion-II (Figure 3(b)).

Motion-I is one of the crucial motions for biped robot walking. When swing legs execute motion in lateral plane and transverse plane, the center of mass (COM) should concentrate on the supporting foot. The side-to-side motion aims to realize the transition from one leg to another one. One step for human corresponds to a cycle for robot, so motion-I should be described as a periodic function. As we all know, sin function is a common periodic function, and it can be used to describe the side-to-side motion.¹⁴ However, only one basic sin function would always lead to incomplete transfer of the COM. When studying on human walking, we know that a whole walking cycle can be divided into a double-support phase (20%) and a single-support phase (80%).¹⁵ Therefore, instead of using one single sin function, we prefer to combine tanh function with the periodicity of sin function, which will meet the requirement of double-support phase and single-support phase of one walk. For side-to-side motion-I, hip roll joint and ankle roll joint are required, thus motion-I can be formulated as

$$\begin{aligned} {}^I\theta_{hip_r}^R &= {}^I\theta_{hip_r}^L = A_I \tanh(2 \cos t) \\ {}^I\theta_{ankle_r}^R &= {}^I\theta_{ankle_r}^L = A_I \tanh(-2 \cos t) \end{aligned}$$

where A_I is related to the maximum distance of COM in lateral plane.

To execute walking in lateral plane, stepping side motion-II is performed by the unloaded leg. The abduction/adduction of unloaded leg in lateral motion only happens in the single-support phase, because in double-support phase, it holds the state of abduction/adduction. So, motion trajectory function of motion-II also uses tanh function, but with half cycle to ensure the stepping side motion is conducted after the transition of COM. Hip roll joint and ankle roll joint are required, thus motion-II can be formulated as

$$\begin{aligned} {}^{II}\theta_{hip_r}^R &= {}^{II}\theta_{hip_r}^L = A_{II} \tanh(2 \sin t) \\ {}^{II}\theta_{ankle_r}^R &= -{}^{II}\theta_{ankle_r}^L = A_{II} \tanh(-2 \sin t) \end{aligned}$$

The unloaded leg will land the floor, when ${}^{II}\theta$ reaches its extremum. The extremum is related to the lateral position of landing foot, and A_{II} is corresponding to the value x of landing foot in Figure 7(a).

Motion types in transverse plane. There are two types of motion in transverse plane, forward motion-III (Figure 3(c)) and rotating motion-IV (Figure 3(d)).

We still use sin function for forwarding motion. Similar to stepping side motion, the forwarding motion also happens after COM transits to supporting foot. In motion-III, six joints of legs are used to walk forward, hip pitch, ankle

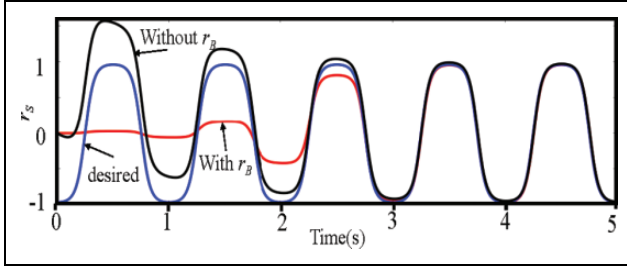


Figure 4. A one-dimensional example radius portrait of a morphed amplitude controlled oscillator. The desired limit cycle is $r_s = \tanh(-2\cos(t))$, which $\theta(r) = \tanh(-2\cos(r))$. For this figure, $c = 2$, $\mu = 1$, $o = 0$, and $\vartheta = 1$. Blue trajectory is the desired trajectory, red trajectory is the output of the one-dimensional oscillator, and the black trajectory is the output without r_B .

pitch, and knee pitch, so motion-III can be formulated as

$$\begin{aligned} \text{III}\theta_{\text{hip}_p}^L &= -\text{III}\theta_{\text{ankle}_p}^L = A_{\text{III}} \sin t \\ \text{III}\theta_{\text{hip}_p}^R &= -\text{III}\theta_{\text{ankle}_p}^R = A_{\text{III}} \sin t \end{aligned}$$

similarly A_{III} is corresponding to the value y of landing foot in Figure 7(a).

To keep upper body upright, the knee joints should meet

$$\text{III}\theta_{\text{knee}_p} = -(\text{III}\theta_{\text{hip}_p} + \text{III}\theta_{\text{ankle}_p})$$

In forward motion, $\text{III}\theta_{\text{hip}_p}$ and $\text{III}\theta_{\text{ankle}_p}$ are reciprocal, so the sum of two values, $\text{III}\theta_{\text{knee}_p}$, is equal to 0.

In the rotation motion, hip yaw pitch joints are used, so motion-IV can be formulated as

$$\text{IV}\theta_{\text{hip}_{yp}}^L = -\text{IV}\theta_{\text{hip}_{yp}}^R = A_{\text{IV}} \sin t$$

similarly, A_{IV} is corresponding to the value ψ of landing foot in Figure 7(a).

Motion types in sagittal plane. There is one type of motion in sagittal plane, lifting motion-V (Figure 3(e)).

Lifting motion makes the foot achieve vertical clearance, which is another crucial motion for walking. Six joints are used for lifting motion: hip pitch, ankle pitch, and knee pitch. So motion-V can be formulated as

$$\begin{aligned} \text{V}\theta_{\text{hip}_p}^L &= \text{V}\theta_{\text{ankle}_p}^L = A_{\text{V}} e^{\cos t} + V_1 \\ \text{V}\theta_{\text{hip}_p}^R &= \text{V}\theta_{\text{ankle}_p}^R = A_{\text{V}} e^{\cos(t+\pi)} + V_2 \\ \text{V}\theta_{\text{knee}_p}^R &= -2A_{\text{V}} e^{\cos(t+\pi)} + V_3 \\ \text{V}\theta_{\text{knee}_p}^L &= -2A_{\text{V}} e^{\cos t} + V_3 \end{aligned}$$

where V_1 , V_2 , and V_3 are constant and related to the initial state.

In the aforementioned five types of motion, side-to-side motion and lifting motion are the basic motion for locomotion. Combining with another three types of motion, these two basic motions can generate any footsteps contained in the reachable region of swing foot. The values of A_{II} , A_{III} , and A_{IV} will control the position of landing foot. Thus, the relationship between parameter of CPG and locomotion is

constructed, and the trajectory functions of each joint are given as

$$\theta_{\text{hip}_r}^R = \text{I}\theta_{\text{hip}_r}^R + \text{II}\theta_{\text{hip}_r}^R \quad (1)$$

$$\theta_{\text{hip}_r}^L = \text{I}\theta_{\text{hip}_r}^L + \text{II}\theta_{\text{hip}_r}^L \quad (2)$$

$$\theta_{\text{ankle}_r}^R = \text{I}\theta_{\text{ankle}_r}^R + \text{II}\theta_{\text{ankle}_r}^R \quad (3)$$

$$\theta_{\text{ankle}_r}^L = \text{I}\theta_{\text{ankle}_r}^L + \text{II}\theta_{\text{ankle}_r}^L \quad (4)$$

$$\theta_{\text{hip}_p}^R = \text{III}\theta_{\text{hip}_p}^R + \text{V}\theta_{\text{hip}_p}^R \quad (5)$$

$$\theta_{\text{hip}_p}^L = \text{III}\theta_{\text{hip}_p}^L + \text{V}\theta_{\text{hip}_p}^L \quad (6)$$

$$\theta_{\text{ankle}_p}^R = \text{III}\theta_{\text{ankle}_p}^R + \text{V}\theta_{\text{ankle}_p}^R \quad (7)$$

$$\theta_{\text{ankle}_p}^L = \text{III}\theta_{\text{ankle}_p}^L + \text{V}\theta_{\text{ankle}_p}^L \quad (8)$$

$$\theta_{\text{knee}_p}^R = \text{III}\theta_{\text{knee}_p}^R + \text{V}\theta_{\text{knee}_p}^R \quad (9)$$

$$\theta_{\text{knee}_p}^L = \text{III}\theta_{\text{knee}_p}^L + \text{V}\theta_{\text{knee}_p}^L \quad (10)$$

$$\theta_{\text{hip}_{yp}}^R = \text{IV}\theta_{\text{hip}_{yp}}^R \quad (11)$$

$$\theta_{\text{hip}_{yp}}^L = \text{IV}\theta_{\text{hip}_{yp}}^L \quad (12)$$

Hence, trajectory regulator in footstep planning for biped robot navigation can be generated.

Central pattern generators

CPG control system is a dynamical system, which is mathematically composed of coupled nonlinear oscillator.¹⁶ There are three common oscillators: two-dimensional nonlinear oscillator (Hopf oscillator), neural network oscillator (Matsuoka oscillator), and dynamical movement primitives (Morphed oscillator). Hopf oscillator can only output a very simple curved line such as sinusoid. Matsuoka oscillator has too many parameters and the process of finding appropriate parameters is a tough task. Compared to the Hopf oscillator and Matsuoka oscillator, morphed oscillator can output arbitrary periodic signal and have a few parameters. So, the morphed oscillator¹⁷ was used in this article.

The start of output from the original morphed oscillator is always unstable, which could lead biped robot to fall; in order to improve its output performance, we define a modified morphed oscillator as

$$\dot{r} = 2\pi\vartheta \quad (13)$$

$$\dot{r}_B = c(1 - r_B)r_B \quad (14)$$

$$\dot{r}_{Si} = \mu \left(2\pi\theta_i(r) + \theta_i(r) \right) r_B - r_{Si} + o \quad (15)$$

where r is the phase, r_B and r_{Si} are, respectively, the radial output of the based oscillator and the i th desired oscillator, r_B controls the method of convergence, c controls the rate of convergence, μ is the radius of the amplitude controlled oscillator, ϑ is the locomotion frequency, $\theta_i(r)/\mu$ defines the shape of the limit cycle of the i th oscillator, $\theta_i(r) = \partial\theta_i(r)/\partial r$, r_{Si} is the joint angle reference for the i th DOF, and o is an added offset and controls the midpoint of the oscillator. There are 12 trajectory functions from formula (1) to (12), so $i = 12$ in this study.

The outstanding feature of the modified oscillator is that it can learn or follow a known attribute. Figure 4 illustrates a one-dimensional example radius portrait of a morphed amplitude controlled oscillator, in which, the blue line is the desired trajectory, whose function is $\theta(r) = \tanh(-2 \cos(r))$. Substituting $\theta(r)$ into formula (15), the red line, outputs of r_{Si} , was obtained. Since r_B controls the method of convergence, there is a transition phase before getting a steady desired trajectory, comparing to the black line. So, these trajectory functions can be used as a desired trajectory to control the leg joints motion.

Adjustable midpoint is another important feature, since the midpoint of the oscillator is related to feedback control in section ‘‘Adaptive walking with feedback.’’ A real-time smooth transition of midpoint is a pressing requirement. Without handling value o , the transition of midpoint is lagging, as shown in Figure 5(a), which would lead robot to tip up because of lacking real-time adjusting for disturbance.

To improve the real-time performance, S function is used.

$$o = \left(\frac{A}{1 + e^{B(t-t_0)}} + 1 \right) o_0$$

where o_0 is the desired changing value, t_0 is the beginning time of midpoint changes, and A and B are an empirical value.

Adding S function can fasten the transition of midpoint, and the result is given in Figure 5(b).

Adaptive walking with feedback

When the biped robot walks forward from flat terrain to incline terrain, without adjusting, the center of gravity will move forward or backward accordingly. Once the position of the center of gravity exceeds the stable support area, the balance will be broken. By adjusting the angle of joints and the step length, the aforementioned situation can be avoided.¹¹ In CPG control system, the oscillator frequency controls the speed of motion, the values of A_{II} , A_{III} , and A_{IV} control the stride of walking, and the midpoint is related to the body position. Building the relationship between these parameters and the feedback signal of sensor will realize biped robot to perform a self-adaption walking on irregular terrains.

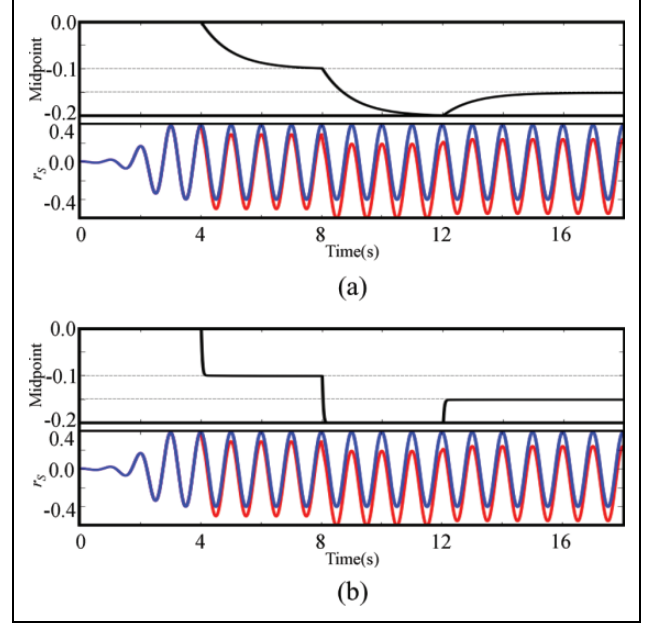


Figure 5. Comparison of midpoint adjustment performance: the value of midpoint (top). Blue curve shows the original curve and the changed curve (bottom). (a) Without S function, $o = 0$, $o = -0.1$, $o = -0.2$, and $o = -0.15$. (b) With S function, $A = 38$, $B = 0.4$.

Normally, the robot body was kept in an upright position when walking on plane. The gyrometer and accelerometer sensor of the robot can monitor the state of the robot body in real time. The value of parameter o , by controlling the oscillator midpoint position of knee joints motion, can adjust the body inclination in sagittal plane. The value of o is set proportionally to the difference between the reference inclination Angle (-0.03 to 0.13 rad) and the current body inclination estimated from the gyrometer sensors, Angle Y . The accelerometer sensors Acc Y forecasts the next inclination. When Angle Y is outside the range of Angle. This relationship can be expressed as

$$o_0 = (\text{Angle} - \text{Angle}Y) + k_2 \text{Acc}Y$$

$$o_2 = o_1 + \left(\frac{A}{1 + e^{B(t-t_0)}} + 1 \right) o_0$$

where o_1 is the original o_2 and o_2 was used to adjust the midpoint of knee pitch trajectory.

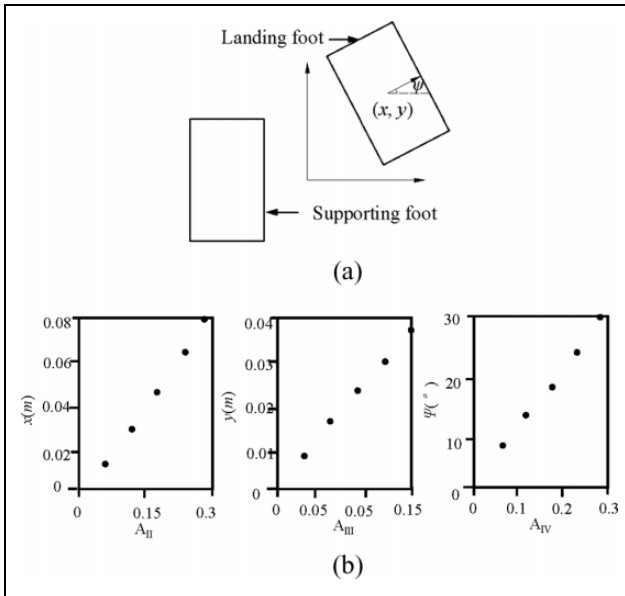
The value of o_2 indicates the slopes of the slope, and the step length will be decreased during up-sloped walking and increased during down-sloped walking. The slope length should change with the slopes of slope. So, o_2 was used to change the value of A_{III}

$$A_{III} = A_{III_0} + \frac{o_2}{S}$$

where A_{III_0} is the original value of parameter A_{III} .

Table 1. Joint values in initial Standinit posture.

Joints	Value	Joints	Value
$\theta_{\text{hip}_p}^R$	-0.4500	$\theta_{\text{hip}_p}^L$	-0.1500
$\theta_{\text{hip}_r}^R$	0.0000	$\theta_{\text{hip}_r}^L$	0.0000
$\theta_{\text{hip}_y}^R$	0.0000	$\theta_{\text{hip}_y}^L$	0.0000
$\theta_{\text{knee}_p}^R$	0.6978	$\theta_{\text{knee}_p}^L$	0.6978
$\theta_{\text{ankle}_r}^R$	0.0000	$\theta_{\text{ankle}_r}^L$	0.0000
$\theta_{\text{ankle}_p}^R$	-0.3489	$\theta_{\text{ankle}_p}^L$	-0.3489

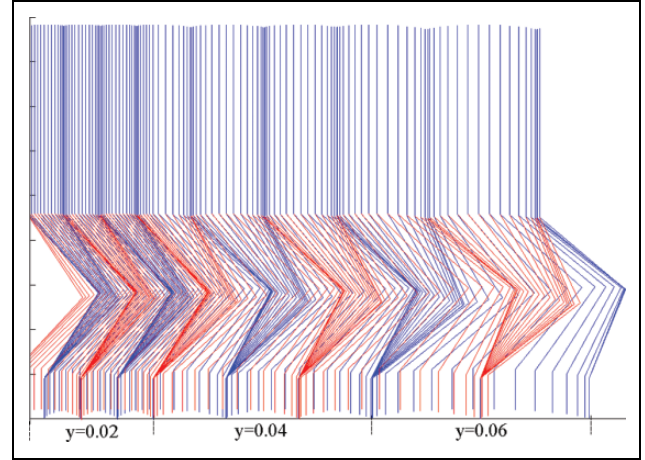
**Figure 6.** A_{II} , A_{III} , and A_{IV} are proportional to x , y , and ψ , respectively. In the experiments, the values are set as 0.25, 0.26, and 111.

Experiments

We validate the CPG control approach both in simulation and on physical robot NAO. Before the experiment, the simulated and physical robots need a definition for initial state. The Choregraphe [SoftBank Robotics, Ver. 2.1.4] software provides a pose library for NAO robot. We borrowed the Standinit Posture¹⁸ from pose library in Choregraphe as initial state, and the joint values in the initial Standinit Posture is given in Table 1. So, $V_1 = -0.3489$, $V_2 = 0.45$, and $V_3 = 0.6978$.

An effective gesture transition trajectory

As mentioned earlier, the position of landing foot is related to the parameters of CPG. This relationship is determined by robot model and the initial state of the robot. The values of A_{II} , A_{III} , and A_{IV} are not relevant to each other and are proportional to x , y , and ψ , respectively, in Figure 6. The values of A_{II} , A_{III} , and A_{IV} are

**Figure 7.** Stick of the NAO model in the case of $A_{II} = 0$, $A_{IV} = 0$, when $A_{III} = 0.068$, $y = 0.02$ m; $A_{III} = 0.1367$, $y = 0.04$ m; and $A_{III} = 0.205$, $y = 0.06$ m.

$$A_{II} = \frac{1}{K_{II}x} \quad (16)$$

$$A_{III} = \frac{1}{K_{III}y} \quad (17)$$

$$A_{IV} = \frac{1}{K_{IV}\psi} \quad (18)$$

where K_{II} , K_{III} , and K_{IV} are constants. By recording the A_{II} , A_{III} , A_{IV} and the x , y , ψ , the proportional relation between A_{II} and x , A_{III} and y , A_{IV} and ψ was proved. In simulation experiment, the values of A_{II} , A_{III} , A_{IV} are 0.26, 0.29, and 167, respectively. Using forward walking as an example, the value y of the landing foot changed significantly with the increase of A_{III} . Figure 7 shows the stick picture of the NAO with A_{III} changing from 0.068 to 0.1367 and then to 0.205. The physical experiment exists gravity and friction that make the values of A_{II} , A_{III} , and A_{IV} different from those in simulation experiment. In physical experiment, the values of A_{II} , A_{III} , and A_{IV} are 0.25, 0.26, and 111, respectively.

Then, the footstep planning and CPG model composed a dual-thread control system. The footstep planning plans in every walking cycle. If the next step is different from current one, the values of A_{II} , A_{III} , and A_{IV} will be changed by principles (16) to (18). In this experiment as demonstrated in Figure 8, the environment was set dynamic and the robot would react to the uncertain environment while approaching to the target red ball. The footstep sequence generated by the footstep planner will be updated with the change of environment information. Since the parameters of CPG were corresponding to the footstep sequence, the robot could walk to the goal.

Adaptive walking on slope terrain with feedback

In this section, slope-adaption walking simulation experiment is conducted in 45 s length and the snapshots are

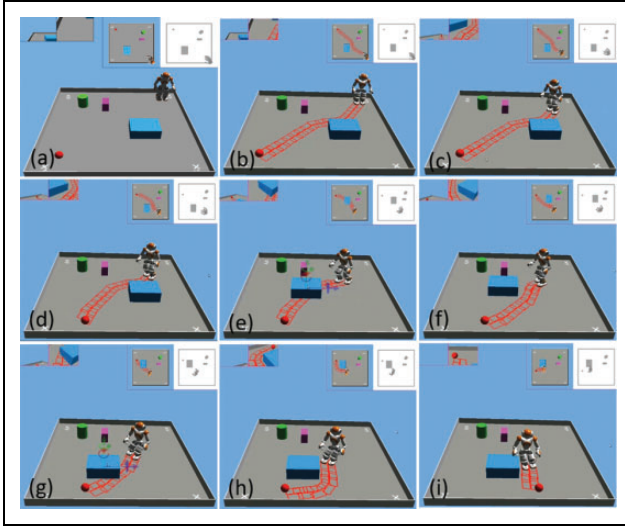


Figure 8. CPG controller generates an effective gesture transition trajectory for sample-based footstep planner. (e)–(g) the position of obstacles was changed and (h)–(i) the position of the target was changed. CPG: central pattern generator.

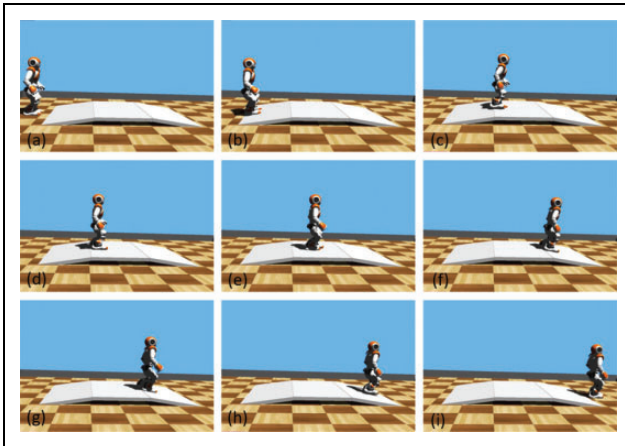


Figure 9. Simulation experiment. (a) and (b) NAO walked from flat terrain to uphill, (c) and (d) NAO walked from uphill to flat terrain, (f) and (g) NAO walked from flat terrain to downhill, (h) and (i) NAO walked from downhill to flat terrain. The dip of the slope is 8.5° .

shown in Figure 9. The robot walked from flat terrain to uphill, then to the flat, to the downhill, and at last to the flat again. The CPG parameters and the corresponding step size for the slope-adaption experiment in simulation are given in Table 2. When the robot walked from the flat terrain to the uphill, the gyro monitors the tip at first. To keep the stability walking for the robot, midpoint of the ankle pitch joints was decreased and the step size turned from 6 cm to 4 cm. When the robot walked from flat terrain to the downhill, midpoint of ankle pitch joints was increased and the step size turned from 6 cm to 8 cm. Figure 10 shows the control signals for the left leg joints in simulation experiment.

Figure 11 shows the change of value of AngleY, which represented the changes of body attitude in y direction. The

Table 2. CPG parameters and corresponding step sizes for the slope-adaption experiment in simulation.

Parameters	Flat terrain	Uphill	Downhill
A_I	0.26	0.26	0.26
A_{II}	0.00	0.00	0.00
A_{III}	0.20	0.14	0.28
A_{IV}	0.00	0.00	0.00
A_V	0.05	0.05	0.05
Step size (cm)	6	4	8

CPG: central pattern generator.

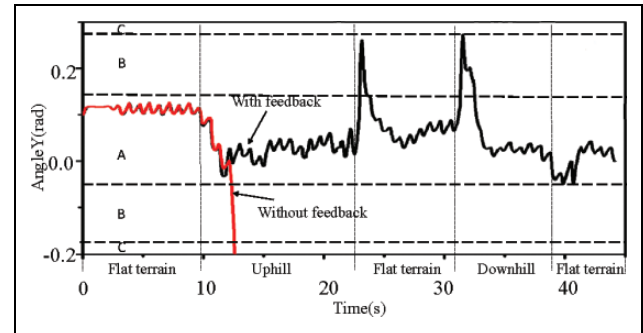


Figure 10. The control signals for the joints of left leg.

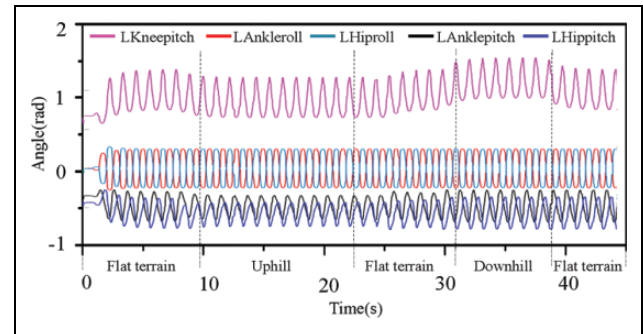


Figure 11. The change of robot attitude feedback. The red curve shows the value of gyro in y direction for the robot walking without feedback and the black curve describes the value of gyro in y direction for robot walking with feedback.

red curve shows the robot walking without any feedback and the black curve shows the robot walking with feedback.

Physical experiment

In the simulated slope walking experiments, the proposed control method was proved feasible. To test the real robots adaptive walking performance, we downloaded the program to a real NAO robot. The robot can walk stably on the slope in which the dip was changed. Figure 12 shows the snapshot of the slope walking experiment. Figure 13(a) and (b) shows the value of gyro in y direction for the robot walking on uphill and downhill. With the change of dip, the value of gyro was in a range. No matter walked on the uphill

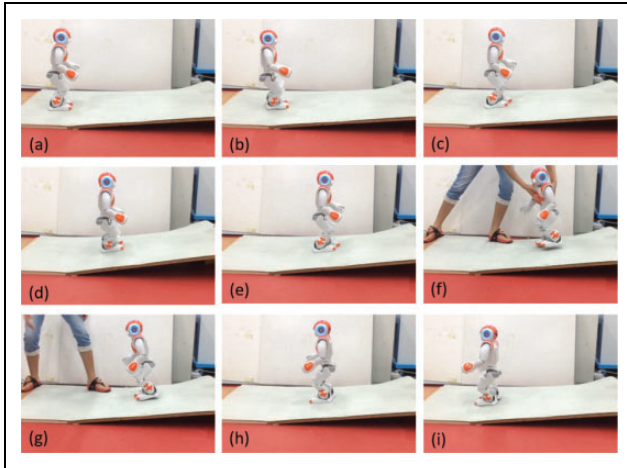


Figure 12. Side-view snapshots of the NAO robot walking on the slope terrain.

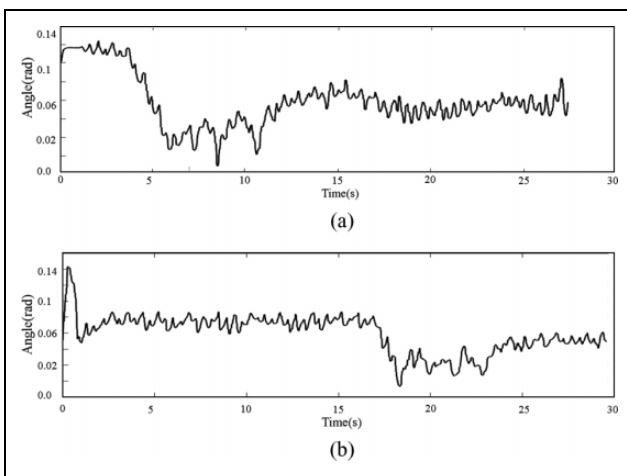


Figure 13. The value of gyro in y direction. (a). Robot walking on uphill and (b) robot walking on downhill.

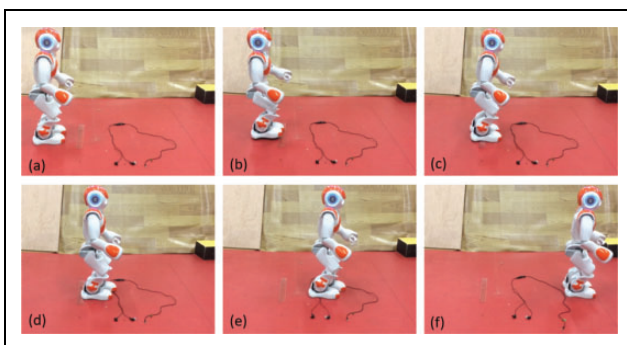


Figure 14. NAO walks on terrain with a ruler and an earphone.

or downhill, the robot walked stably. With the proposed control method, the robot also can walk on the terrain with some tiny obstacles. The snapshots of walking on tiny obstacles experiment are shown in Figure 14.

Conclusion and future work

In this work, the CPG-joint control method was presented to replace ISP to offer a new method of gesture transition trajectory in footstep planning for biped robot navigation and realize a self-adaption walking for irregular terrains.

The advantage of the proposed method is that a whole walking motion was decomposed into five periodic motion types, and two of them, motion-I and II, are basic motion types for walking motion. By combining two basic motion types with another three motions, it can easily reach any walking motion, for example, walking forward, walking lateral, and turning. Then, the joint motion trajectories were generated to build the trajectory regulator according to the attributes of motion types. This relationship between joint motion trajectories and the position of swing foot is built successfully. This relationship makes landing foot to reach anywhere in the reachable region. The amount of parameters of CPG is small, in which three parameters are adjustable, and the rest are constant. At last, the feedback control ensures the robot walking on irregular terrains, such as walking on unknown sloped terrains and flat floor with tiny obstacles. The simulator and physical experiments proved the feasibility of the proposed CPG control method.

Our future interests include (1) optimizing the CPG control method from energy efficiency and building more complex feedback control, (2) applying the proposed method to more challenging tasks, such as terrain with larger slope, and (3) applications on other types of biped robots.

Declaration of conflicting interests

The author(s) declared no potential conflicts of interest with respect to the research, authorship, and/or publication of this article.

Funding

The author(s) disclosed receipt of the following financial support for the research, authorship, and/or publication of this article: This work was supported by National Science Foundation of China (51305436, 61403368), Guangdong Natural Science Foundation for Distinguished Young Scholars (2015A030306020), Major Project of Guangdong Province Science and Technology Department (2014B090919002), Fundamental Research Program of Shenzhen (JCYJ20140901003939038, JCYJ20140417113430639), Research Project of Shenzhen (GJHS20160331190459402), Shenzhen High-level Oversea Talent Program (KQJSCX20160301144248) and Youth Innovation Promotion Association, Chinese Academy of Sciences (No. 2015301).

References

1. Kuffner J, Nishiwaki K, Kagami S, et al. Footstep planning among obstacles for biped robots. In: *IEEE international conference intelligent robots and systems*, Maui, Hawaii, October 29–November 3, 2001. 2001, pp.500–505. IEEE.
2. Chestnutt J, Lau M, Cheung G, et al. Footstep planning for the Honda ASIMO humanoid. *IEEE international conference on*

- robotics and automation*, Orlando, Florida, May 15-19, 2006. 2006, pp.629–634. IEEE.
3. Ayaz Y, Munawar K, Malik M, et al. Humanlike approach to footstep planning among obstacles for humanoid robots. *Int J Human Robot* 2007; 4(1): 125–149.
 4. Xia Z, Liu L, Xiong J, et al. Design aspects and development of humanoid robot THBIP-2. *Robotica* 2008; 26(1): 109–116.
 5. Xia Z, Chen G, Xiong J, et al. A random sampling-based approach to goal-directed footstep planning for humanoid robots. In: *IEEE/ASME international conference on advanced intelligent mechatronics*, Suntec, Singapore, July 14-17, 2009. 2009, pp.168–173. IEEE.
 6. Xia Z, Xiong J and Chen K, Global navigation for humanoid robots using sampling-based footstep planner. *IEEE/ASME Trans Mech* 2011; 16, 716–723.
 7. Fairhall A and Bialek W. Adaptive spike coding. In: Arbib M (ed.) *The handbook of brain theory and neural networks*. 2nd ed. Cambridge: MIT Press, 2002, pp.90–94.
 8. Olivira M, Matos V, Santos CP, et al. Multi-objective Parameter CPG Optimization for Gait Generation of a Biped Robot. In: *IEEE International conference on robotics and automation*, Karlsruhe, Germany, May 6-10, 2013. 2013, pp.3130–3135. IEEE.
 9. Nassour J, Henaff P, Benouezdou F, et al. Multi-layered multi-pattern CPG for adaptive locomotion of humanoid robots. *Biol Cybern* 2014; 108(3); 291–303.
 10. Endo G, Nakanishi J, Morimoto J, et al. Experimental studies of a neural oscillator for biped locomotion with QRIO. In: *International conference on robotics and automation*, Barcelona, Spain, April 18-22, 2005. 2005, pp.596–602, IEEE.
 11. Kai TS and Chang HH. CPG-based control design for bipedal walking on unknown slope surfaces. In: *IEEE international conference on robotics and automation*, Hong Kong, China, May 31-June 7, 2014. 2014, pp. 5109–5114. IEEE.
 12. Liu C, Wang D, and Chen Q. Central pattern generator inspired control for adaptive walking of biped robots. *IEEE Trans Syst Man Cybern* 2013; 43(5): 1206–1215.
 13. Aldebarab Documents, Nao-Actuator & Sensor list [Internet]. 2016. Available from: http://doc.aldebaran.com/2-1/family/nao_dcm/actuator_sensor_names.html#actuator-sensor-list-nao. (2016, accessed 9 August 2016).
 14. Morimoto J, Endo G, Nakanishi J, et al. A biologically inspired biped locomotion strategy for humanoid robots: modulation of sinusoidal patterns by a coupled oscillator model. *IEEE Trans Robot* 2008; 24: 185–191.
 15. Huang Q, Kajita S, Koyachi N, et al. A high stability, smooth walking pattern for a biped. In: *IEEE international conference on robotics and automation*, Detroit, Michigan, May 10-15, 1999. 1999, pp.65–71. IEEE.
 16. Yu J, Tan M, Chen J, et al. A Survey on CPG-inspired control models and system implementation. *Neural Netw Learn Syst* 2014; 25: 441–456.
 17. Ajallooeian M, Kieboom JVD, Mukovskiy A, et al. A general family of morphed nonlinear phase oscillators with arbitrary limit cycle shape. *Physica D* 2013; 263: 41–56.
 18. Aldebarab Documents, Pose library panel [Internet]. Available from: http://doc.aldebaran.com/2-1/software/choregraphe/panels/pose_library_panel.html. (2016, accessed 9 August 2016)